HHS Public Access

Author manuscript

Mol Psychiatry. Author manuscript; available in PMC 2022 January 15.

Published in final edited form as:

Mol Psychiatry. 2021 October ; 26(10): 5690–5701. doi:10.1038/s41380-021-01150-w.

Transmission of cerebral amyloid pathology by peripheral administration of misfolded Aβ aggregates.

Rodrigo Morales, PhD[1,2,*,†], **Javiera Bravo-Alegria, PhD**[1,3,*], **Ines Moreno-Gonzalez, PhD**[1,2,4], **Claudia Duran-Aniotz, PhD**[1,3,5], **Nazaret Gamez**[1,4], **George Edwards III, PhD**[1], **Claudio Soto, PhD**[1,3,†]

[1]Mitchell Center for Alzheimer's disease and related brain disorders. Department of Neurology. The University of Texas Health Science Center at Houston. 6431 Fannin St. Houston, Texas 77030, USA.

[2]Centro integrativo de biología y química aplicada (CIBQA). Universidad Bernardo O'Higgins. Santiago, Chile.

[3]Universidad de los Andes, Facultad de Medicina. Av. San Carlos de Apoquindo 2200, Las Condes, Santiago, Chile.

[4]Department of Cell Biology, Faculty of Sciences, University of Malaga-IBIMA, 29010 Malaga, Spain. Networking Research Center on Neurodegenerative Diseases (CIBERNED).

[5]Center for Social and Cognitive Neuroscience (CSCN), School of Psychology, Universidad Adolfo Ibáñez, Santiago de Chile, Chile.

Abstract

Previous reports showed that brain Aβ amyloidosis can be induced in animal models by exogenous administration of pre-formed aggregates. To date, only intra-peritoneal and intra-venous administrations are described as effective means to peripherally accelerate brain Aβ amyloidosis by seeding. Here, we show that cerebral accumulation of Aβ can be accelerated after exposing mouse models of Alzheimer's disease (AD) to Aβ seeds by different peripheral routes of administration, including intra-peritoneal and intra-muscular. Interestingly, animals receiving drops of brain homogenate laden with Aβ seeds in the eyes were efficiently induced. On the contrary, oral administration of large quantities of brain extracts from aged transgenic mice and AD patients did not have any effect in brain pathology. Importantly, pathological induction by peripheral administration of Aβ seeds generated a large proportion of aggregates in blood vessels, suggesting vascular transport. This information highlights the role of peripheral tissues and body fluids in AD-related pathological changes.

[†]Correspondence should be addressed to R.M. (Rodrigo.MoralesLoyola@uth.tmc.edu; +1 (713) 500-7442) or C.S. (Claudio.Soto@uth.tmc.edu; +1 (713) 500-7086).

[*]These authors contributed equally to this work

AUTHOR CONTRIBUTIONS

R.M. and C.S. designed the experiments. R.M., J.B-A., I.M-G., C.D-A. and G.E.III performed the experimental work. R.M., J.B-A., I.M-G and C.S. analyzed the data. R.M. wrote the manuscript. All authors reviewed and approved the final version of this article.

COMPETING FINANCIAL INTERESTS

The authors declare no competing financial and competing non-financial interests.

INTRODUCTION

Alzheimer's disease (AD), the most common form of dementia worldwide, is characterized by the accumulation of misfolded amyloid-β (Aβ) and tau proteins in the brain [1, 2]. As such, AD is classified as a protein misfolding disorder (PMD), a group of clinically diverse diseases caused by the accumulation of abnormally folded proteins in specific tissues [3]. Aβ aggregates are considered as the earliest pathological abnormality in AD, which might trigger the subsequent changes leading to neurodegeneration and disease. In humans and animal models, accumulation of misfolded Aβ causes tau pathology, synaptic dysfunction, cell death, and cognitive decline [4–11]. Among the different misfolded Aβ species present in the AD brain, oligomers are attributed to participate in the initial stages of seeding [12], subsequently leading to a decrease in neurogenesis and increased neuronal death [13]. Mutations in the Aβ precursor protein (APP) and proteins assisting in Aβ production are responsible for all familial AD cases [14, 15].

Several reports demonstrate that Aβ misfolding can be induced by seeding in a similar way as described for infectious prions (reviewed in [16, 17]). The intra-cerebral (i.c.) administration of misfolded Aβ in susceptible rodent models accelerate brain amyloidosis [18–20], induce pathological changes in all-or-none systems [21, 22], display a dose-dependent effect [23], and differentially propagate conformational strains [24, 25]. Experimental transmission of brain Aβ misfolding has also been achieved in non-transgenic primates [26, 27]. Importantly, the prion-like behavior of misfolded Aβ explains very well how these particles accumulate overtime and spread along different brain structures [28]. Besides i.c. infusions, brain Aβ amyloidosis can be induced by the intra-peritoneal (i.p.) administration of seeding-competent aggregates [29]. However, this specific peripheral challenge was less efficient than i.c. injections, similarly as observed in prion diseases [30–32]. The induction of cerebral amyloid angiopathy (CAA) in Aβ-treated mice by the i.p. route suggest an important involvement of the vasculature in transporting these molecules from the periphery to the central nervous system (CNS) [29, 33]. This hypothesis is further supported by colocalization of peripheral misfolded Aβ aggregates with specific blood components [33]. Although the seeding mechanism governing Aβ and prion spread are similar at the brain level, they differ at the periphery as oral, intra-venous, intra-nasal and intra-ocular administration of seeds failed to induce Aβ deposition in the CNS [34]. Importantly, the peripheral routes mentioned above are efficient in transmitting prion diseases [35–37].

Studying the role of peripheral tissues and fluids in brain Aβ deposition may be critical for the development of diagnostic methods and new therapies aimed to halt AD progression. Here, we evaluated whether the administration of biologically active Aβ seeds through various peripheral routes accelerate pathological changes in the brains of mice models of cerebral amyloidosis.

MATERIALS AND METHODS

Mice.

Tg2576 mice [38] were used in these experiments (54% males, n=4–12). These mice start displaying scattered brain amyloid deposits between 8–10 months as described in publications from our group [23, 39] and others [40]. Mice subjected to injections or a single oral gavage were treated at 50 days old. Repeated administrations (eye drops and repeated oral gavages) in different groups of animals started at the same age (specific details below). I.c. administered mice were sacrificed at 285 days old. Animals injected by peripheral routes were sacrificed at 300 days old. Animals were housed in standard conditions (22°C, 12 hours light/dark cycles). All experimental procedures were in accordance with the regulations of the Center of Laboratory Animal Medicine and Care (CLAMC) and the Animal Welfare Committee (AWC) of The University of Texas Health Science Center at Houston.

Inocula.

a) Tg2576-derived: 10% w/v brain homogenates from aged (18- to 20-months-old) Tg2576 mice were prepared in Phosphate Buffer Saline (PBS, MP Biomedicals, Santa Ana, CA, USA) supplemented with a cocktail of protease inhibitors (PI, Roche Diagnostics GmbH, Mannheim, Germany). Resulting samples were pooled, aliquoted, snap-frozen in liquid nitrogen and stored at −80°C until use. This inoculum was previously characterized in a Aβ seeds titration study [23]. b) *Human-derived*: The brain extract from an AD patient (temporal cortex) was prepared similarly as described above. The AD sample was derived from a clinically confirmed AD case (male, 84 years old) displaying abundant neuritic and cored plaques and some diffuse aggregates (Braak stage IV, Supplemental Figure 1). Use of human samples was approved by the Institutional Review Board (IRB) of The University of Texas Health Science Center at Houston.

Intra-cerebral injections.

Anesthetized mice (n=5) were injected with 20 μL of the Tg2576-derived inoculum into the hippocampus (10 μL per brain hemisphere, AP, −1.8 mm; L, ±1.8 mm; DV, −1.8 mm) using aseptic techniques with a stereotaxic apparatus.

Intra-peritoneal injections.

For intra-peritoneal injections (n=6), isofluorane anesthetized mice were inoculated with 100 μL of the Tg2576-derived inoculum into the peritoneal cavity using a tuberculin syringe (gauge 27 1/2 G).

Eye drops.

For administration of eye drops, 5 μL of the Tg2576-derived inoculum were dropped into each eye of isoflurane narcotized 50 days old mice (n=5) using a 10 μL pipette tip. Animals were restrained by the tail for approximately 1 minute after treatment and then returned into their cages. The same procedure was repeated weekly two additional times.

Oral gavages (*per os*, p.o.).

For p.o. administrations, a total of 1 mL of Tg2576-derived inoculum was introduced into the stomach of hand restrained mice (n=4) using a feeding needle. Additional groups of mice were either treated 5 times per week for four weeks (20 doses in total) with 500 μL of 10% w/v brain homogenate from an AD patient (prepared as described above, n=9), or PBS (n=12).

Intra-muscular injections.

For i.m. inoculations, 50 μL of Tg2576-derived inoculum were injected with a tuberculin syringe (gauge 27 1/2 G) in each animal's thigh (n=6).

Non-treated animals.

Additional untreated animals (n=6) were used as controls.

Immunohistochemistry and ThS staining.

Brains were immersion-fixed in 10% formalin, then dehydrated and embedded in paraffin. Serial 10 μm-thick sagittal sections were cut using a microtome. For Aβ staining, brain slices were previously treated with 85% formic acid for 5 min at room temperature for antigen retrieval followed by a blocking step with 3% H_2O_2/10% methanol solution in PBS. Then, brain sections were incubated overnight with mouse anti-Aβ 4G8 antibody (Biolegend, Cat#800710) diluted 1:1,000 in PBS/0.02% Triton-X 100 (Sigma, St. Louis, MO, USA) and then incubated for 1 h with sheep anti-mouse IgG–Horseradish Peroxidase (HRP) secondary antibody (GE Healthcare, Little Chalfont, UK) diluted at a 1:500 ratio. Peroxidase reaction was visualized using 3,3′-Diaminobenzidine (DAB) Kit (Vector Laboratories, Burlingame, CA, USA) following manufacturer's instructions. Stained sections were dehydrated in graded ethanol, cleared in xylene, and cover-slipped with DPX mounting medium (Innogenex, San Ramon, CA, USA). Brain tissue slices from an AD patient were counterstained with hematoxylin. ThS staining was performed in brain slices consecutive to 4G8 stained sections. For this, tissue slices were incubated with a ThS (Sigma, St. Louis, MO, USA) solution (0.1% ThS in 50% ethanol) for 15 min after deparaffinization. After incubation, sections were washed for 2 min in 80% ethanol, dehydrated and cover-slipped.

Image analyses.

For quantification of Aβ burden, brain slices were examined under a DMI6000B microscope (Leica, Buffalo Grove, IL, USA) and image analysis was performed as previously described [23, 41, 42]. Briefly, Aβ deposits in pictures taken with a 5X objective from cortical and hippocampal areas were quantified using the ImageJ software (National Institutes of Health, Bethesda, MD, USA). Aβ burden was expressed as a percentage of the area stained by the 4G8 antibody versus the total area analyzed. Five tissue slices per animal were analyzed (one every 100 μm). The specific brain regions used in each measurement are described in Supplemental Figure 2. For specific quantification of vascular Aβ deposition, slices stained with 4G8 were quantified for blood vessel associated staining by manually deselecting parenchymal plaques from the same images used to measure total Aβ load, similarly

as described before [43]. For Aβ lesion profile (three brain slices every tenth), images of olfactory bulb (OB), frontal cortex (FC), parietal cortex (PC), occipital cortex (OC), hippocampus (HP), thalamus (TH), caudate/putamen and striatum (ST) and cerebellum (CB) were taken with a 2.5X objective, and image analysis was performed as described above. The percentage of lesion was defined as the area stained with anti-Aβ antibody versus the total area analyzed and normalized as a percentage for each tissue sliced analyzed. Plaque density was calculated by counting the total number of plaques in cortex and hippocampus divided by the total area analyzed in each brain region. Personnel performing these analyses were blind to the identity of the samples.

Quantification of insoluble Aβ species by ELISA.

Brain homogenates were prepared at 10% w/v in PBS 1X supplemented with PI, as described above. Insoluble Aβ was isolated and characterized as described previously [41]. Briefly, 200 μL of brain extracts were ultracentrifuged at 32,600 rpm for 1 h at 4°C using a 42.2 Ti rotor (Beckman-Coulter, Brea, CA). Supernatants were collected, snap-frozen in liquid nitrogen, and pellets resuspended by pipetting and sonication in 200 μL of 70% formic acid (Fisher Scientific, Waltham, MA, USA). Samples were ultracentrifuged for 30 min at the same conditions described above, and supernatants were collected. Formic acid fractions were diluted 20 times in volume using 1M Tris buffer, pH 11 (Sigma-Aldrich, St. Louis, MO) in order to neutralize pH. The $A\beta_{42}$ concentration of the formic acid soluble fractions was measured with Human $A\beta_{42}$ ELISA kit (Invitrogen, Carlsbad, CA, USA). The assays were developed following manufacturer's recommendations. Samples were read on an ELISA reader (EL800 BIO-TEK, BioTek, Winooski, VT, USA) at 450 nm. Personnel performing these analyses were blind to the identity of the samples.

Statistical Analyses.

Number of animals in each group was based in our previous experience using mice treated with infectious prions and availability of inoculum (oral gavages). Kolmogorov-Smirnov or Skewness-Kurtosis statistic tests were used to confirm normal distribution of the data. Next, 1-way ANOVA followed by a multiple comparison test (Tukey) or student's t-test were used to analyze differences between groups. The values were expressed as means ± Standard Error of the Mean (SEM). Data was analyzed using the Graph Pad Prism software (GraphPad, La Jolla, CA, USA), version 5.0. *$p < 0.05$, **$p < 0.01$, ***$p < 0.001$. Statistical differences were considered significant for values of $p < 0.05$. In order to appreciate the treatment effect in individual mice, we defined an attack rate threshold emulating experiments in which prion infection produced disease only in some of the animals treated [32, 44]. To define the attack rate thresholds, the limit was set at 3 standard deviations (3σ) over the mean of untreated controls. Individual values above the attack rate thresholds were defined as positive for seeded amyloid induction. No inclusion/exclusion criteria or randomization methods were applied to experimental groups.

RESULTS

Administration of Aβ seeds by peripheral routes accelerates brain amyloidosis

50-days-old Tg2576 mice were exposed, by different routes, to brain extracts from 18- to 20-months-old Tg2576 mice harboring large quantities of Aβ deposits. Routes of administration included i.c., i.p., intra-muscular (i.m.) and *per os* (p.o.). Additionally, we tested eye drops (e.d.) to assess the effect of direct ocular contact with Aβ aggregates on brain amyloidosis. Volume and estimated amounts of Aβ administered varied depending on the route to allow maximum exposure (Table 1). Due to the non-invasive nature of the e.d. administration and the unknown amount of brain homogenate absorbed through this route, three weekly e.d. doses were performed instead of one as for all other routes (summarized in Table 1 and Supplemental Figure 3). Animals were sacrificed at either 285 (i.c.) or 300 (all other routes) days old. At these ages, untreated mice show little Aβ deposits in their brains, as previously reported [23].

Aβ deposition was initially assessed by immunohistochemistry (IHC) in the cortex and the hippocampus, the brain areas where Aβ deposits are more abundant in this model [23, 38]. As expected, untreated mice sacrificed at 300 days old displayed low levels of amyloid deposition (Figures 1A and 1B). Aβ burden values in these mice were similar to the ones observed in animals injected with brain homogenate from wild type mice (data not shown) or PBS [23]. As expected, the cortex and hippocampus of animals i.c. injected with brain extracts from aged Tg2576 mice generated massive deposition of Aβ amyloid at the experimental end point (Figures 1A and 1B). In addition, we confirmed previous results obtained by Eisele *et al.* [29] by showing that i.p. administration of Aβ-laden materials is able to induce cerebral amyloid deposition (Figures 1A and 1B). The administration of Aβ seeds by two other peripheral routes, i.m. and e.d., also accelerated brain amyloidosis (Figures 1A and 1B). As explained in Material and Methods section, we defined an attack rate threshold to appreciate the treatment effect in individual mice. This analysis is reminiscent of many experiments involving infectious prions where disease is observed in only a fraction of the animals treated [32, 44]. Here, the attack rate threshold was defined as three standard deviations over the average value of the untreated control group (dotted red line in Figure 1B). We observed that 4 out of 6 i.m. treated mice showed significantly higher levels of Aβ deposits compared to controls (Figure 1B). Surprisingly, mice treated with e.d. (a non-invasive way of administration) showed a complete attack rate, with average Aβ burden levels similar to the ones seen in the i.m. group. On the contrary, none of the p.o. treated Tg2576 mice displayed burden values above the attack rate threshold. This is noteworthy as the amount of material administered was substantially higher compared to all other groups (Table 1). Negative results in the p.o. group were further confirmed by showing that twenty repetitive administrations of an AD brain extract (harboring large quantities of Aβ deposits) in young Tg2576 mice did not modify the extent of brain pathology (Supplemental Figure 1).

In regards to amyloid distribution in the brains of mice receiving seeds by peripheral routes, we did not observe significant differences in cortex and hippocampus (Supplemental Figure 4). However, the patterns of deposition in mice receiving seeds by the i.m. route were erratic.

This is reflected by the incomplete attack rates observed in this group and non-uniform patterns of amyloid deposition across the brain of individual animals (Supplemental Figure 5).

Ocular and i.p. Aβ seeds administration are the most efficient peripheral routes for seeding

To best compare the extent of Aβ seeding by different routes, we calculated the ratio between Aβ burden values obtained for each animal and the estimated amount of seeds administered as evaluated by ELISA (Table 1). As expected, i.c. administration was at least 25 times more efficient than all other peripheral administrations (Figure 1C). Nevertheless, IHC is known to possess low sensitivity and unable to detect non-clustered/soluble Aβ aggregates. For that reason, the opposite brain hemispheres from the same experimental and control mice were homogenized and levels of PBS-insoluble Aβ were analyzed by ELISA. In addition of being more sensitive, this test allowed us to assess the Aβ content in preparations involving all brain structures in a more quantitative manner. Insoluble Aβ levels largely confirmed the IHC analyses, only slightly differing in the i.m. administrations (attack rate of 3 out of 6, Figure 2A). When ELISA values were normalized for the estimated amount of seeds administered, we observed that e.d. treated mice contained higher quantities of insoluble Aβ compared to the i.m and i.p groups (Figure 2B). It is important to highlight the non-invasive nature of this route, as well as the overestimation of seeds entering into the eye. However, these results suggest e.d. as an efficient mean of extra-neural Aβ transmission.

Another way to assess seeding efficiency is to compare the resulting Aβ burden in each experimental group with that of untreated animals sacrificed at different time points. We have previously done this analysis for Tg2576 mice i.c. challenged with different amounts of Aβ seeds [23]. In that specific case, pathological features were shown to be accelerated in over a year for the most concentrated inoculum [23]. By plotting Aβ burden versus time for these untreated animals (9–19 months old, Table 2 and Figure 3), i.c. administrations were calculated to accelerate cerebral Aβ amyloid deposition over 9 months (Table 2). Moreover, the i.m. and e.d groups revealed levels of Aβ deposits similar to 14-months-old untreated mice, indicating the acceleration of brain amyloidosis equivalent to 4 months (Table 2 and Figure 3). Among all peripheral administration routes, i.p. showed the highest net efficiency with an equivalency of Aβ burden similar to untreated mice sacrificed at around 16 months old (Table 2 and Figure 3).

A high proportion of seeded Aβ deposits are associated with vascular tissue.

Infectious prions are known to reach the brain either by direct transport through the blood brain barrier [45] or by retrograde transport through peripheral nerves after peripheral replication [44, 46]. For Aβ, previous reports show that seeds placed in the peritoneal cavity can be found associated to monocytes up to 1 week after administration [33]. Additionally, Aβ deposition induced by the i.p. administration of seeds was importantly associated with blood vessels [29, 33]. Amyloid deposits naturally generated by Tg2576 mice are mostly located in the brain parenchyma and vascular deposition is negligible when present. To better understand the contribution of CAA in seeded animals, we quantified the burden of Aβ deposits associated with vascular and meningeal vessels in all our experimental and

control groups, using previously described methodologies [43]. Our results demonstrate that all seeded animals, with the sole exception of the p.o. groups, developed vascular Aβ deposits (Figure 4A). Quantification of these protein deposits showed that the amount of vascular aggregates followed the total amount of Aβ induced by each treatment (Figure 4B). Indeed, i.c. administrations displayed the highest amount of deposits compared to all other groups. However, considering that the total burden for each route group was different, we normalized the vascular Aβ deposition readings to the total aggregation induced in each case. Interestingly, we observed that the contribution of vascular deposition in peripherally induced Aβ pathology (i.p. and e.d.) was higher and significantly different compared to i.c. administration (Figure 4C). This data suggests that peripherally administered Aβ aggregates reach the brain by vascular routes and from there seed parenchymal amyloid deposition.

Different peripheral routes generate distinct brain seeding tropisms.

Considering the differential vascular vs. parenchymal extent of Aβ deposition induced by the administration of preformed seeds through distinct routes, we investigated for potential differences on the brain areas affected by Aβ pathology. As a baseline, we used brains from untreated 19- to 21-months-old Tg2576 mice and compared their amyloid pathology distribution with that of the experimental groups. Aggregates in old/untreated mice were concentrated in the cortical areas (mostly frontal cortex), hippocampus and olfactory bulb. Other brain regions, such as the striatum, thalamus and cerebellum presented considerably lower Aβ pathology (Figure 5A and 5E). A similar deposition profile was observed for animals receiving seeds by e.d (Figure 5B and 5F). Conversely, the pathology induced by i.p. (Figure 5C and 5G) and i.c. (Figure 5D and 5H) administration of seeds displayed different brain tropisms (additional pictures of micés brains from the e.d. and i.p. groups are provided in Supplemental Figure 6). The i.p. group generated a significantly higher amount of deposits in the olfactory bulb, while i.c. (intra-hippocampal) injections of seeds shifted the aggregates to the hippocampus, as expected [23]. In addition, we observed that the latter route generated a lower proportion of aggregates in the frontal cortex. The i.m. administration was not included in this analysis due to their incomplete attack rate and the high variability observed in induced mice (Supplemental Figure 5).

Seeds administered by different routes generated a wide variety of aggregates.

Gross examination of brain tissues revealed clear morphological differences among the Aβ deposits generated by seeding. Aged untreated Tg2576 mice (19–21 months old) manifested compact plaques comprising minor diffuse pathology (Figure 6A, first panel). Untreated control animals and experimental mice receiving Aβ seeds by the p.o. route (both sacrificed at 300 days old) showed scattered small and compact plaques, especially in the cortex and the hippocampus (Figure 6B and not shown). Compact and larger deposits compared to the latter two groups were observed for animals receiving e.d (Figure 6C). Mice from the i.m. group displayed Aβ aggregates with a compact core and surrounded by more diffuse deposition (Figure 6D). Distinct from all other groups, i.p. and i.c. injected animals generated large and diffuse (fleecy-like) aggregates (Figures 6E and 6F, respectively). To further confirm our observations, we stained consecutive tissue slices with thioflavin S (ThS), a dye extensively characterized to bind compact amyloid structures [47]. Plaques from the p.o. and e.d. groups displayed comparable co-localization of ThS staining when

compared with anti-Aβ staining (Figures 6H and 6I, respectively), similar to aged untreated Tg2576 mice (Figure 6G). Consistent with IHC, only the core of the plaques in the i.m. group showed ThS staining (Figure 6K). On the contrary, little or no ThS signal was observed for most of the Aβ aggregates in the i.p. and i.c. groups (Figures 6K and 6L, respectively). Importantly, the aggregates associated with blood vessels in all seeded mice were positive for ThS (Supplemental Figures 7A and 7B). Other than vascular deposits, the i.c. group developed ThS-reactive plaques only in the needle track (Supplemental Figures 7C and 7D). This data suggests that Aβ seeding can generate different pathological features depending on the route of administration.

DISCUSSION

Several proteins associated with neurodegenerative diseases, such as α-synuclein, tau, Aβ, among others, have been experimentally shown to share features with disease-associated prions [3, 17, 48]. After administration of pre-formed seeds in suitable animal models, these proteins induce or accelerate pathological features in a prion-like manner [16, 17, 48]. Aside from prionopathies, only Amyloid-A (AA) amyloidosis in cheetahs has been proven to be transmissible between individuals in non-experimental conditions [49]. Data from grafted cells in Parkinson's disease patients [50], and Aβ amyloidogenesis in young individuals receiving dura transplants [51, 52] or administration of human growth hormone [53, 54] suggest the possibility of clinically relevant inter-cell and inter-individual transmission of protein misfolding. At minimum, the current evidence supports the idea that the prion-like behavior of misfolded proteins is at the core of the intra-individual spread of pathogenic units from cell-to-cell and from brain region-to-brain region [48, 55, 56]. By comparing the pathological induction of misfolded protein aggregates with the characteristics of *bona fide* prions, we have gained a better understanding of how neurodegenerative diseases progress and may help to design new strategies for disease intervention and diagnosis.

Our results showing that the exogenous administration of Aβ aggregates by different routes can propagate amyloid pathology into the brain highlight the role of peripheral Aβ in the progression of brain amyloidosis. Previous reports suggest that brain and peripheral Aβ concentrations are at equilibrium [57, 58]. This equilibrium is maintained by the ability of Aβ to cross the blood-brain barrier in both directions. Importantly, peripherally administered Aβ binds pre-formed plaques present in the brain [58, 59]. Confirming previous observations made by Jucker and colleagues [29], we observed that a single administration of Aβ seeds in the peritoneal cavity increases amyloid deposition in Tg2576 mice. Additionally, we described that other means of administration such as i.m. injections and e.d. also accelerated brain Aβ pathology. These results partially contradict a previously published report showing that peripheral routes other than i.p were unable to modify brain amyloidosis [34]. This discrepancy may be due to the different mouse model used (Tg2576 vs. APP23), the source of inoculum (Tg2576 vs. APP23 brain extracts), and/or the different incubation periods in each case (which has been shown to be a key determinant for Aβ seeding *in vivo* [60]). Regarding the ocular route, the previous report tested intra-ocular injection of minute amounts of brain extracts (1 μL of a 10% brain homogenate). In our experimental approach, a non-invasive strategy was used by placing a larger quantity of seeds directly onto the eye surface. Surprisingly, e.d. was the most efficient peripheral route

of administration when pathological induction was made relative to the amount of seeds administered. This result takes a higher relevance considering that from the 30 μL placed onto the eyes (5 μL per eye each week) it is likely that only a small fraction of it was internalized. I.m. administration of seeds was also efficient in accelerating changes in the brain, albeit the incomplete attack rates obtained. All of these results strongly suggest that misfolded Aβ present in peripheral tissues may have an effect in the progression of brain AD-associated pathological changes. Conversely, the administration of high quantities of seeds by oral gavages did not generate changes in the brain, even when two sources of inoculum and two different dosages were tested.

The strong association of seeded aggregates with blood vessels suggests that aggregates administered in the periphery reached the brain through the circulation. Actually, one experiment using a mouse model lacking Aβ in the periphery suggests that seeds administered by the i.p. route exert their effects by directly reaching the brain [33]. This information supports the idea that blood is an important vector for the spread of Aβ seeds between peripheral tissues and the brain. Our data confirms previous results showing that seeded aggregation (by i.c. or i.p. routes) promotes the appearance of these type of aggregates [28, 29, 61, 62]. Moreover, normalized vascular pathology data for two out of three of the peripheral routes tested (i.p. and e.d.) was significantly increased compared to the one observed in mice receiving seeds directly in the brain. This data support the idea that peripheral seeds initially promote aggregation in vascular structures, subsequently inducing pathology in the brain parenchyma. This is plausible considering Aβ aggregates as dynamic entities ranging from small oligomers to large fibrils. In that sense, small/seeding-competent Aβ oligomers could be released from these initial pools of vascular amyloids and spread pathology in a prion-like fashion to the brain parenchyma. Nevertheless, the possibility that Aβ aggregates replicate in peripheral tissues and undergo retrograde transport by peripheral nerves, as described for prion diseases [63], has not yet been disproven. This is especially relevant for our results involving e.d. administrations, since eyes are highly innervated organs with direct neural connectivity to the brain. On the contrary, the administration of high quantities of Aβ seeds by the p.o route suggest that aggregates are degraded in the gastrointestinal tract or are unable to cross the epithelial layers. Additional experiments are needed to understand how peripherally applied Aβ reaches the brain to spread protein misfolding.

In addition to the vascular tropism observed for seeded Aβ deposits, we tested whether exogenous administration of misfolded Aβ by different routes changed the distribution of the aggregates across the brain. Tg2576 mice spontaneously accumulate Aβ mostly in the cerebral cortex and hippocampus, with little deposition observed in other areas. We previously showed that the distribution of Aβ aggregates can be shifted by the site of i.c. injection [23], with aggregates appearing in a larger extent in the injected area. This conclusion is further supported by the results of the current experiments. On the other hand, peripheral routes led to varying pathological profiles. While e.d. treated mice caused a similar brain distribution of Aβ aggregates when compared to aged Tg2576, i.p. administrations resulted in different outcomes with significant amyloidosis in the olfactory bulb. It is likely that the different tropism of Aβ deposition by distinct routes might be due to differential brain entry of Aβ aggregates in e.d. and i.p. routes. We are currently

investigating the mechanisms governing the entry of Aβ aggregates after different means of administration to further understand these unexpected outcomes.

Aβ deposits in AD patients are heterogeneous and easily differentiated by their morphology and reactivity against amyloid-specific dyes, such as Congo Red and ThS [47, 64]. Among the various distinct types of Aβ deposits, it is possible to distinguish neuritic, mature, diffuse and fleecy plaques, as well as synaptic diffuse and intra-cellular aggregates [64]. The presence and proportion of these aggregates may vary between individuals and the brain regions analyzed. In this study, we discovered that the route of administration of seeds influenced the types of deposits generated in the brain. Importantly, seeded aggregates were different compared to what is observed in aged Tg2576 mice and resembled more closely the pathological features found in the brain of AD patients [64]. We are currently investigating the biological relevance of each type of aggregate generated by seeding in the context of inflammation, synapto- and cell-toxicity, and tissue damage.

It is important to mention that the experiments described in this article were done using brain extracts containing high quantities of misfolded Aβ and that the amount administered was variable depending of the route of administration (we used the maximum volumes allowed per route). Whether the differential pathological features generated by seeding are due to the variable quantities of misfolded Aβ administered will be explored in future studies.

The data presented in this article highlight the role of peripheral tissues and blood in the progression of brain Aβ amyloidogenesis. This subject acquires more relevance considering reports suggesting that peripheral administration of cadaveric pituitary preparations (supposedly containing Aβ aggregates) may seed Aβ misfolding in the brain [53, 54]. Considering the data presented in this article, other medical procedures such as corneal transplants (tissues known to accumulate misfolded Aβ [65]) should be revisited for possible inter-individual transmission of biologically active seeds. Future epidemiological studies designed to directly address these questions may be useful to either confirm or discard the inter-individual transmission of Aβ misfolding. Besides the implications of this phenomenon in public health, our results highlight the important contribution of peripheral Aβ in the spreading of brain amyloidosis in AD. The identification Aβ aggregates in different tissues and fluids may serve as an efficient biomarker to diagnose the disease. In the same line, removal of Aβ species from the periphery may alter the stability of brain deposits in a beneficial manner, opening new avenues for therapeutic interventions.

Supplementary Material

Refer to Web version on PubMed Central for supplementary material.

ACKNOWLEDGMENTS

The authors would like to thank Mrs. Andrea Flores-Ramirez for animal care and genotyping. This work was supported by grants from the NIH (RF1 AG059321) to C.S. and R.M., the Alzheimer's Association (MNIRGD-12–243075 and NIRGD-15–363554 to R.M., NIRP-12–257323 to I.M-G and AARG-591107 to CDA), grants from ANID (ANID/FONDEF ID20I10152 and ANID/FONDECYT 1210622) to CDA and a grant from The Mitchell Foundation (to C.S).

REFERENCES

1. Mrcpsych B, Jones E, Ballard C, Gauthier S, Corbett A, Brayne C, et al. Alzheimer's disease. Lancet 2011;377:1019–1031. [PubMed: 21371747]
2. Querfurth HW, LaFerla FM. Alzheimer's Disease. N Engl J Med 2010;362:329–344. [PubMed: 20107219]
3. Soto C. Unfolding the role of protein misfolding in neurodegenerative diseases. Nat Rev Neurosci 2003;4:49–60. [PubMed: 12511861]
4. Oddo S, Caccamo A, Shepherd JD, Murphy MP, Golde TE, Kayed R, et al. Triple-transgenic model of Alzheimer's Disease with plaques and tangles: Intracellular Aβ and synaptic dysfunction. Neuron 2003. 2003. 10.1016/S0896-6273(03)00434-3.
5. Götz J, Chen F, Van Dorpe J, Nitsch RM. Formation of neurofibrillary tangles in P301L tau transgenic mice induced by Aβ42 fibrils. Science (80-) 2001. 2001. 10.1126/science.1062097.
6. Lewis J, Dickson DW, Lin WL, Chisholm L, Corral A, Jones G, et al. Enhanced neurofibrillary degeneration in transgenic mice expressing mutant tau and APP. Science (80-) 2001. 2001. 10.1126/science.1058189.
7. He Z, Guo JL, McBride JD, Narasimhan S, Kim H, Changolkar L, et al. Amyloid-β plaques enhance Alzheimer's brain tau-seeded pathologies by facilitating neuritic plaque tau aggregation. Nat Med 2018. 2018. 10.1038/nm.4443.
8. Bucciantini M, Calloni G, Chiti F, Formigli L, Nosi D, Dobson CM, et al. Prefibrillar amyloid protein aggregates share common features of cytotoxicity. J Biol Chem 2004. 2004. 10.1074/jbc.M400348200.
9. Demuro A, Mina E, Kayed R, Milton SC, Parker I, Glabe CG. Calcium dysregulation and membrane disruption as a ubiquitous neurotoxic mechanism of soluble amyloid oligomers. J Biol Chem 2005;280:17294–17300. [PubMed: 15722360]
10. Shankar GM, Li S, Mehta TH, Garcia-Munoz A, Shepardson NE, Smith I, et al. Amyloid-beta protein dimers isolated directly from Alzheimer's brains impair synaptic plasticity and memory. NatMed 2008;14:837–842.
11. Wang HW, Pasternak JF, Kuo H, Ristic H, Lambert MP, Chromy B, et al. Soluble oligomers of β amyloid (1–42) inhibit long-term potentiation but not long-term depression in rat dentate gyrus. Brain Res 2002. 2002. 10.1016/S0006-8993(01)03058-X.
12. Katzmarski N, Ziegler-Waldkirch S, Scheffler N, Witt C, Abou-Ajram C, Nuscher B, et al. Aβ oligomers trigger and accelerate Aβ seeding. Brain Pathol 2020. 2020. 10.1111/bpa.12734.
13. Ziegler-Waldkirch S, d′Errico P, Sauer J, Erny D, Savanthrapadian S, Loreth D, et al. Seed-induced Aβ deposition is modulated by microglia under environmental enrichment in a mouse model of Alzheimer's disease. EMBO J 2018. 2018. 10.15252/embj.201797021.
14. Goate A, Chartier-Harlin MC, Mullan M, Brown J, Crawford F, Fidani L, et al. Segregation of a missense mutation in the amyloid precursor protein gene with familial Alzheimer's disease. Nature 1991;349:704–706. [PubMed: 1671712]
15. Schellenberg GD, Bird TD, Wijsman EM, Orr HT, Anderson L, Nemens E, et al. Genetic linkage evidence for a familial Alzheimer's disease locus on chromosome 14. Science (80-) 1992;258:668–671.
16. Morales R, Callegari K, Soto C. Prion-like features of misfolded Aβ and tau aggregates. Virus Res 2015;207:106–112. [PubMed: 25575736]
17. Jucker M, Walker LC. Self-propagation of pathogenic protein aggregates in neurodegenerative diseases. Nature 2013;501:45–51. [PubMed: 24005412]
18. Kane MD, Lipinski WJ, Callahan MJ, Bian F, Durham RA, Schwarz RD, et al. Evidence for Seeding of β-Amyloid by Intracerebral Infusion of Alzheimer Brain Extracts in β-Amyloid Precursor Protein-Transgenic Mice. J Neurosci 2000;20:3606–3611. [PubMed: 10804202]
19. Meyer-Luehmann M, Coomaraswamy J, Bolmont T, Kaeser S, Schaefer C, Kilger E, et al. Exogenous induction of cerebral beta-amyloidogenesis is governed by agent and host. Science (80-) 2006;313:1781–1784.

20. Baker HF, Ridley RM, Duchen LW, Crow TJ, Bruton CJ. Induction of beta (A4)-amyloid in primates by injection of Alzheimer's disease brain homogenate. Comparison with transmission of spongiform encephalopathy. Mol Neurobiol 1994;8:25–39. [PubMed: 8086126]
21. Morales R, Duran-Aniotz C, Castilla J, Estrada LD, Soto C. De novo induction of amyloid-β deposition in vivo. Mol Psychiatry 2012;17:1347–1353. [PubMed: 21968933]
22. Rosen RF, Fritz JJ, Dooyema J, Cintron AF, Hamaguchi T, Lah JJ, et al. Exogenous seeding of cerebral $β$-amyloid deposition in $β$APP-transgenic rats. J Neurochem 2012;120:660–666. [PubMed: 22017494]
23. Morales R, Bravo-Alegria J, Duran-Aniotz C, Soto C. Titration of biologically active amyloid-$β$ seeds in a transgenic mouse model of Alzheimer's disease. Sci Rep 2015;5:9349. [PubMed: 25879692]
24. Watts JC, Condello C, Stöhr J, Oehler A, Lee J, DeArmond SJ, et al. Serial propagation of distinct strains of A$β$ prions from Alzheimer's disease patients. Proc Natl Acad Sci U S A 2014;111:10323–10328. [PubMed: 24982139]
25. Stöhr J, Condello C, Watts JC, Bloch L, Oehler A, Nick M, et al. Distinct synthetic A$β$ prion strains producing different amyloid deposits in bigenic mice. Proc Natl Acad Sci U S A 2014;111:10329–10334. [PubMed: 24982137]
26. Baker HF, Ridley RM, Duchen LW, Crow TJ, Bruton CJ. Evidence for the experimental transmission of cerebral beta-amyloidosis to primates. Int J Exp Pathol 1993;74:441–454. [PubMed: 8217779]
27. Gary C, Lam S, Hérard AS, Koch JE, Petit F, Gipchtein P, et al. Encephalopathy induced by Alzheimer brain inoculation in a non-human primate. Acta Neuropathol Commun 2019. 2019. 10.1186/s40478-019-0771-x.
28. Ye L, Hamaguchi T, Fritschi SK, Eisele YS, Obermuller U, Jucker M, et al. Progression of Seed-Induced Abeta Deposition within the Limbic Connectome. Brain Pathol 2015. February 2015.
29. Eisele YS, Obermüller U, Heilbronner G, Baumann F, Kaeser SA, Wolburg H, et al. Peripherally applied Abeta-containing inoculates induce cerebral beta-amyloidosis. Science (80-) 2010;330:980–982.
30. Fraser H, Dickinson AG. Studies of the lymphoreticular system in the pathogenesis of scrapie: the role of spleen and thymus. J Comp Pathol 1978;88:563–573. [PubMed: 101558]
31. Bartz JC, Dejoia C, Tucker T, Kincaid AE, Bessen RA. Extraneural prion neuroinvasion without lymphoreticular system infection. J Virol 2005;79:11858–11863. [PubMed: 16140762]
32. Kincaid AE, Bartz JC. The nasal cavity is a route for prion infection in hamsters. J Virol 2007;81:4482–4491. [PubMed: 17301140]
33. Eisele YS, Fritschi SK, Hamaguchi T, Obermuller U, Fuger P, Skodras A, et al. Multiple factors contribute to the peripheral induction of cerebral beta-amyloidosis. JNeurosci 2014;34:10264–10273. [PubMed: 25080588]
34. Eisele YS, Bolmont T, Heikenwalder M, Langer F, Jacobson LH, Yan ZX, et al. Induction of cerebral β-amyloidosis: Intracerebral versus systemic Aβ inoculation. Proc Natl Acad Sci U S A 2009. 2009. 10.1073/pnas.0903200106.
35. Kimberlin RH, Walker CA. Pathogenesis of mouse scrapie: patterns of agent replication in different parts of the CNS following intraperitoneal infection. J R Soc Med 1982;75:618–624. [PubMed: 6809940]
36. Bartz JC, Kincaid AE, Bessen RA. Retrograde transport of transmissible mink encephalopathy within descending motor tracts. J Virol 2002;76:5759–5768. [PubMed: 11992004]
37. Llewelyn CA, Hewitt PE, Knight RSG, Amar K, Cousens S, Mackenzie J, et al. Possible transmission of variant Creutzfeldt-Jakob disease by blood transfusion. Lancet 2004;363:417–421. [PubMed: 14962520]
38. Hsiao K, Chapman P, Nilsen S, Eckman C, Harigaya Y, Younkin S, et al. Correlative Memory Deficits, Aβ Elevation, and Amyloid Plaques in Transgenic Mice. Science (80-) 1996;274.
39. Morales Rodrigo, Claudia Duran-Aniotz Javiera Bravo-Alegria, Estrada Lisbell D., Shahnawaz Mohammad, Hu Ping-Ping, Kramm Carlos, Diego Morales-Scheihing AU& CS. Infusion of blood

from mice displaying cerebral amyloidosis accelerates amyloid pathology in animal models of Alzheimer's disease. Acta Neuropathol Commun 2020;8:213. [PubMed: 33287898]

40. Kawarabayashi T, Younkin L, Saido T, Shoji M, Ashe K, Younkin S. Age-dependent changes in brain, CSF, and plasma amyloid î2 protein in the Tg2576 transgenic mouse model of Alzheimer's disease. J Neurosci 2001. 2001. 10.1523/JNEUROSCI.21-02-00372.2001.
41. Duran-Aniotz C, Morales R, Moreno-Gonzalez I, Hu PP, Fedynyshyn J, Soto C. Aggregate-depleted brain fails to induce A$β$ deposition in a mouse model of Alzheimer's disease. PLoS One 2014;9:e89014. [PubMed: 24533166]
42. Duran-Aniotz C, Morales R, Moreno-Gonzalez I, Hu PP, Soto C. Brains from non-Alzheimer's individuals containing amyloid deposits accelerate Abeta deposition in vivo. Acta NeuropatholCommun 2013;1:76.
43. Wilcock DM, Gordon MN, Morgan D. Quantification of cerebral amyloid angiopathy and parenchymal amyloid plaques with Congo red histochemical stain. Nat Protoc 2006. 2006. 10.1038/nprot.2006.277.
44. Kimberlin RH, Walker CA. Pathogenesis of mouse scrapie: Effect of route of inoculation on infectivity titres and dose-response curves. J Comp Pathol 1978. 1978. 10.1016/0021-9975(78)90059-2.
45. Urayama A, Morales R, Niehoff ML, Banks WA, Soto C. Initial fate of prions upon peripheral infection: half-life, distribution, clearance, and tissue uptake. FASEB J 2011;25:2792–2803. [PubMed: 21555356]
46. Fraser H, Dickinson AG. Pathogenesis of scrapie in the mouse: the role of the spleen. Nature 1970;226:462–463. [PubMed: 4985820]
47. Kelényi G. Thioflavin S fluorescent and congo red anisotropic stainings in the histologic demonstration of amyloid. Acta Neuropathol 1967. 1967. 10.1007/BF00688089.
48. Soto C Transmissible proteins: expanding the prion heresy. Cell 2012;149:968–977. [PubMed: 22632966]
49. Zhang B, Une Y, Fu X, Yam J, Ge F, Yao J, et al. Fecal transmission of AA amyloidosis in the cheetah contributes to high incidence of disease. Proc Natl Acad Sci U S A 2008. 2008. 10.1073/pnas.0800367105.
50. Kordower JH, Chu Y, Hauser RA, Freeman TB, Olanow CW. Lewy body-like pathology in long-term embryonic nigral transplants in Parkinson's disease. Nat Med 2008;14:504–506. [PubMed: 18391962]
51. Frontzek K, Lutz MI, Aguzzi A, Kovacs GG, Budka H. Amyloid-β pathology and cerebral amyloid angiopathy are frequent in iatrogenic Creutzfeldt-Jakob disease after dural grafting. Swiss Med Wkly 2016. 2016. 10.4414/smw.2016.14287.
52. Kovacs GG, Lutz MI, Ricken G, Ströbel T, Höftberger R, Preusser M, et al. Dura mater is a potential source of Aβ seeds. Acta Neuropathol 2016;131:911–923. [PubMed: 27016065]
53. Jaunmuktane Z, Mead S, Ellis M, Wadsworth JDF, Nicoll AJ, Kenny J, et al. Evidence for human transmission of amyloid-$β$ pathology and cerebral amyloid angiopathy. Nature 2015;525:247–250. [PubMed: 26354483]
54. Ritchie DL, Adlard P, Peden AH, Lowrie S, Le Grice M, Burns K, et al. Amyloid-β accumulation in the CNS in human growth hormone recipients in the UK. Acta Neuropathol 2017;134:221–240. [PubMed: 28349199]
55. Soto C, Estrada L, Castilla J. Amyloids, prions and the inherent infectious nature of misfolded protein aggregates. Trends Biochem Sci 2006;31:150–155. [PubMed: 16473510]
56. Walker L, Levine H, Jucker M. Koch's postulates and infectious proteins. Acta Neuropathol 2006;112:1–4. [PubMed: 16703338]
57. DeMattos RB, Bales KR, Cummins DJ, Dodart J-C, Paul SM, Holtzman DM. Peripheral anti-A antibody alters CNS and plasma A clearance and decreases brain A burden in a mouse model of Alzheimer's disease. Proc Natl Acad Sci 2001. 2001. 10.1073/pnas.151261398.
58. Mackic JB, Bading J, Ghiso J, Walker L, Wisniewski T, Frangione B, et al. Circulating amyloid-β peptide crosses the blood-brain barrier in aged monkeys and contributes to Alzheimer's disease lesions. Vascul Pharmacol 2002. 2002. 10.1016/S1537-1891(02)00198-2.

59. Ghilardi JR, Catton M, Stimson ER, Rogers S, Walker LC, Maggio JE, et al. Intra-arterial infusion of [125I]A beta 1–40 labels amyloid deposits in the aged primate brain in vivo. Neuroreport 1996. 1996.

60. Hamaguchi T, Eisele YS, Varvel NH, Lamb BT, Walker LC, Jucker M. The presence of Abeta seeds, and not age per se, is critical to the initiation of Abeta deposition in the brain. Acta Neuropathol 2012;123:31–37. [PubMed: 22101366]

61. Ye L, Fritschi SK, Schelle J, Obermüller U, Degenhardt K, Kaeser SA, et al. Persistence of Aβ seeds in APP null mouse brain. Nat Neurosci 2015.

62. Maclean CJ, Baker HF, Ridley RM, Mori H. Naturally occurring and experimentally induced β-amyloid deposits in the brains of marmosets (Callithrix jacchus). J Neural Transm 2000. 2000. 10.1007/s007020070060.

63. Shearin H, Bessen RA. Axonal and transynaptic spread of prions. J Virol 2014;88:8640–8655. [PubMed: 24850738]

64. Thal DR, Walter J, Saido TC, Fändrich M. Neuropathology and biochemistry of Aβ and its aggregates in Alzheimer's disease. Acta Neuropathol 2015.

65. Moncaster JA, Pineda R, Moir RD, Lu S, Burton MA, Ghosh JG, et al. Alzheimer's disease amyloid-beta links lens and brain pathology in Down syndrome. PLoS One 2010. 2010. 10.1371/journal.pone.0010659.

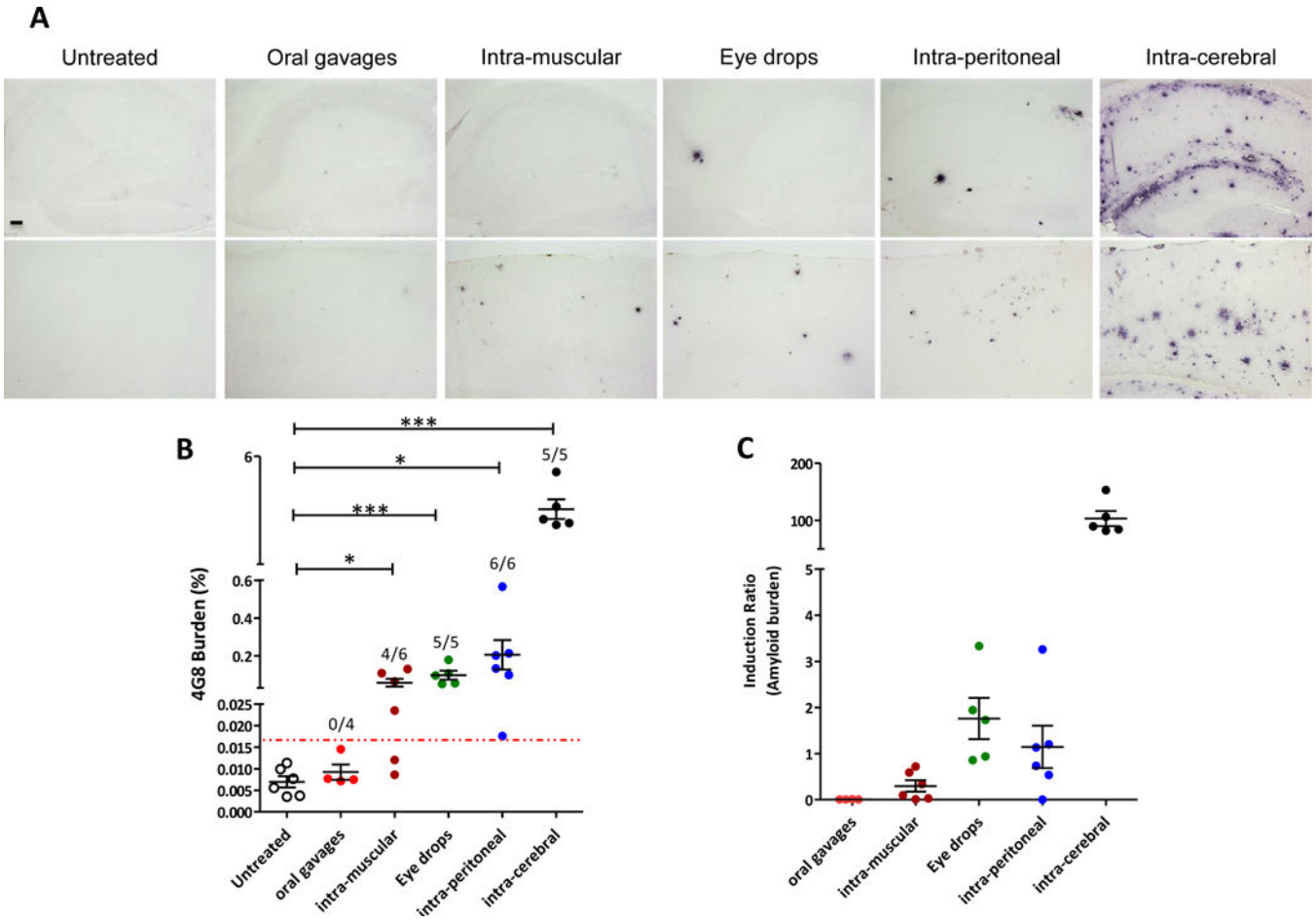

Figure 1. Tg2576 mice challenged with Aβ seeds by different routes developed accelerated brain amyloidosis.

(A) Representative pictures of hippocampi (upper panels) and cerebral cortices (lower panels) of untreated and treated mice with Aβ seeds by different routes of administration. Scale bar in the top left panel represents 100 μm and applies to all panels. **(B)** Aβ burden in cortices and hippocampi was measured in tissue slices, as explained in Material and Methods. Aβ burden is expressed as a percentage for the area stained by the 4G8 anti-Aβ antibody versus the whole area analyzed. Attack rate (ratio depicted at the top of each group) was defined as the fraction of animals having burden values 3σ over the average of untreated animals (red punctuated line). **(C)** Induction ratio was calculated by taking the burden area obtained in (B) and dividing by the estimated amount of Aβ seeds administered in each case (as depicted in Table 1). For (B), lines within the groups represent the mean average of amyloid burden values ± standard error of the mean (SEM). Statistical differences in amyloid burden for each group were measured by Student's t-test with respect to the "Untreated" (negative control) group. *$p < 0.05$, ***$p < 0.001$.

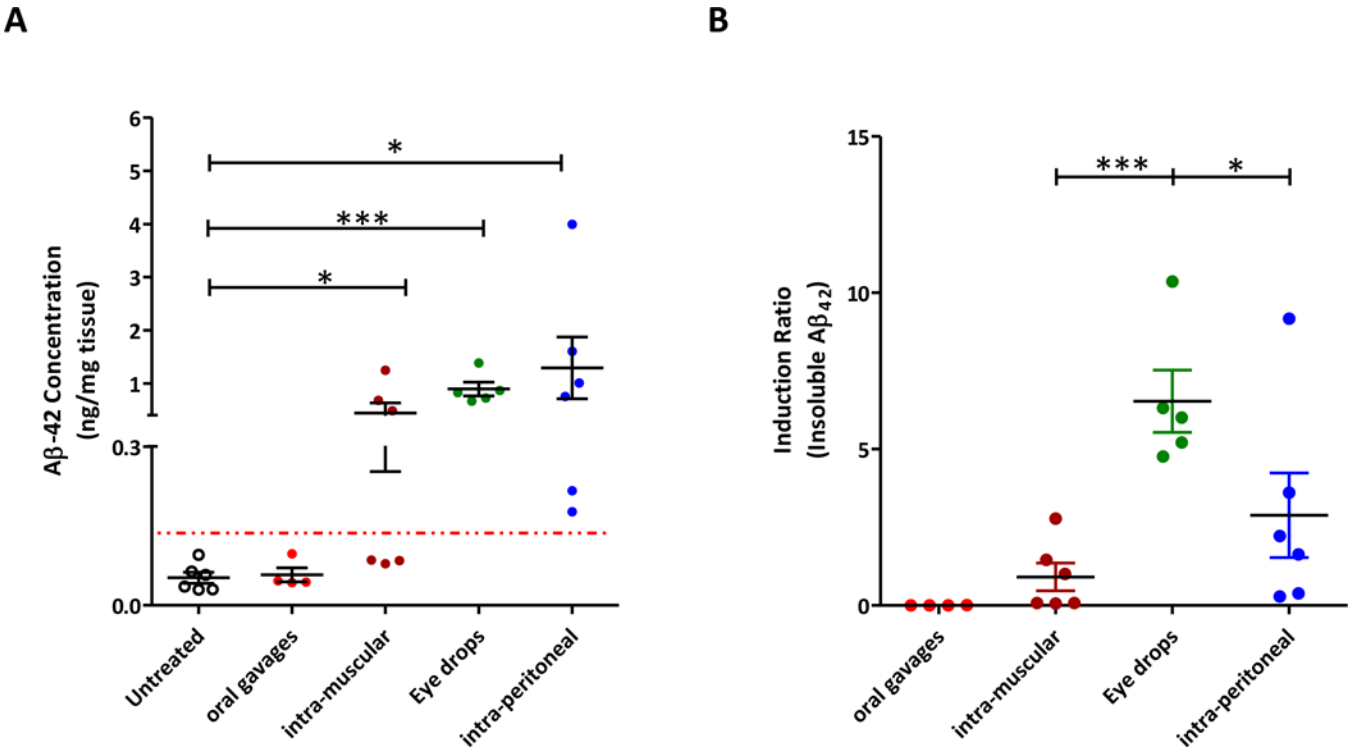

Figure 2. Evaluation of insoluble $A\beta_{42}$ levels in Tg2576 mice receiving biologically active seeds by peripheral routes.

(A) PBS-insoluble Aβ was fractionated as described in Material and Methods and measured by ELISA. A threshold to define attack rates was defined for values 3σ over the average of the untreated control group (red punctuated line). **(B)** Induction ratio was calculated by taking the individual values obtained in (A) and dividing them by the estimated amount of Aβ seeds administered in each case (as depicted in Table 1). Lines within the groups represent the mean average ± SEM. Statistical differences in Aβ concentration values (A) in each group were measured by Student's t-test with respect to the "Untreated" (negative control) group. Statistical analyses in (B) were performed by 1-way ANOVA followed by Dunn's multiple comparison test. *$p < 0.05$, ***$p < 0.001$.

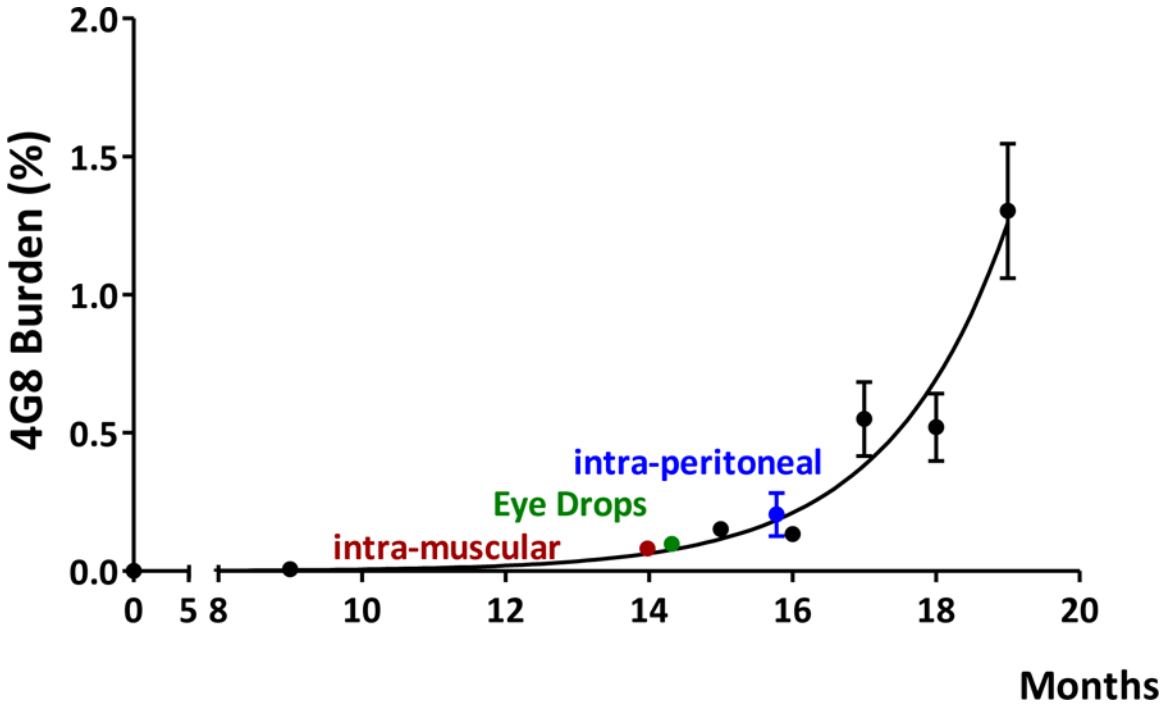

Figure 3. Comparison of Aβ burden between seeded and untreated Tg2576 sacrificed at different time points.

Untreated Tg2576 mice were sacrificed at different time points (ranging from 9 to 19 months old) and Aβ burden was measured by image analysis in cortex and hippocampus (black dots). An Aβ deposition curve was generated using this data (black line) and values for experimental (Aβ seeded) animals were extrapolated on it (colored dots). Vertical lines represent the mean average ± SEM. Data in this figure is expressed in months as untreated mice were sacrificed at the respective months with a ± difference of 5 days.

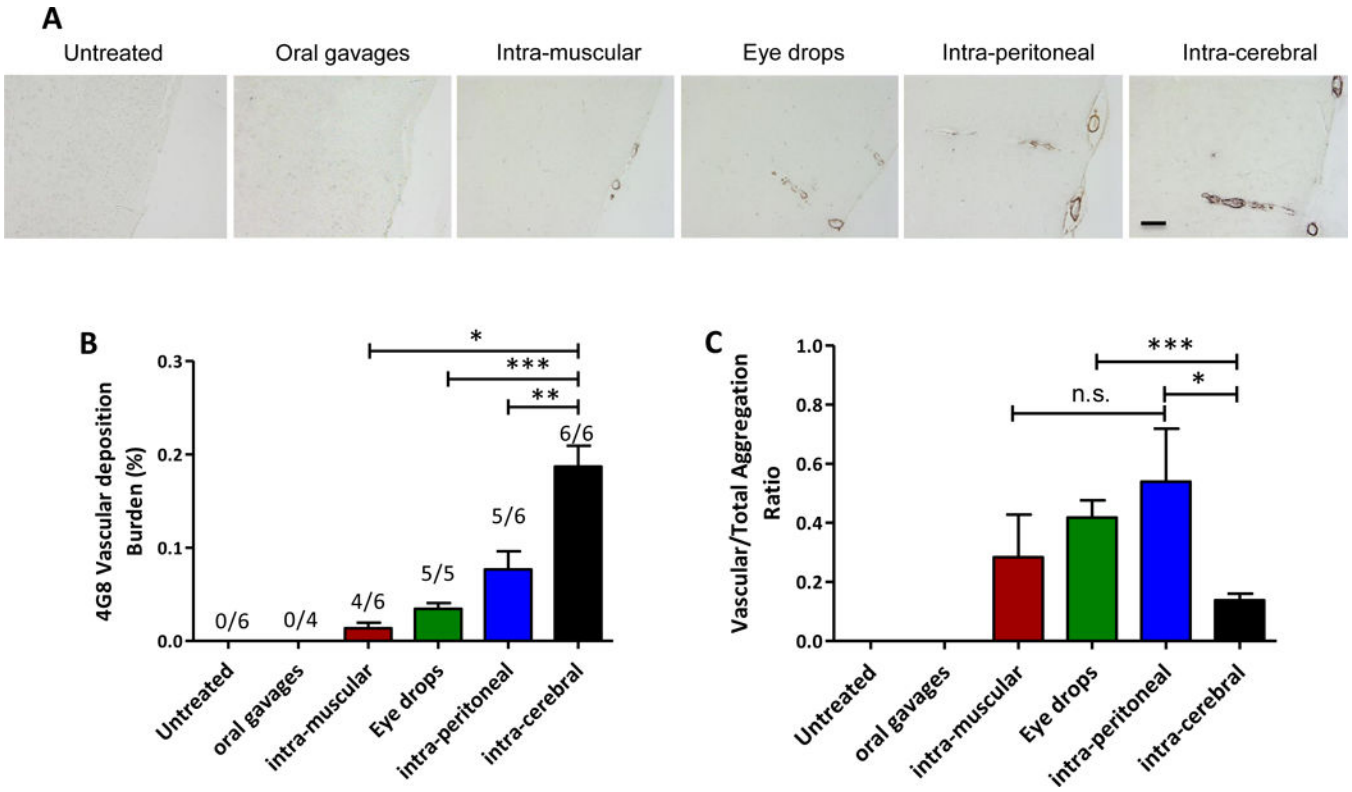

Figure 4. Seeded Aβ deposits in the brain of Tg2576 mice are highly associated with blood vessels.

(A) Representative pictures of mice from different groups showing vascular anti-Aβ (4G8) staining. Scale bar in the right panel represents 100 μm and applies to all panels. **(B)** Net vascular deposition was measured for each experimental group in brain cortices and hippocampi by image analysis and data expressed as burden (%). Numbers at the top of each column represent the number of animals showing vessel-associated aggregates versus the total number of animals analyzed. **(C)** Individual values in (B) were divided by the total Aβ deposition found for each animal as depicted in Figure 1B to calculate the extent of vascular deposition in each case. For (B) and (C), lines at the top of each column represent standard errors. *$p < 0.05$; **$p < 0.01$; ***$p < 0.001$; n.s., not significant.

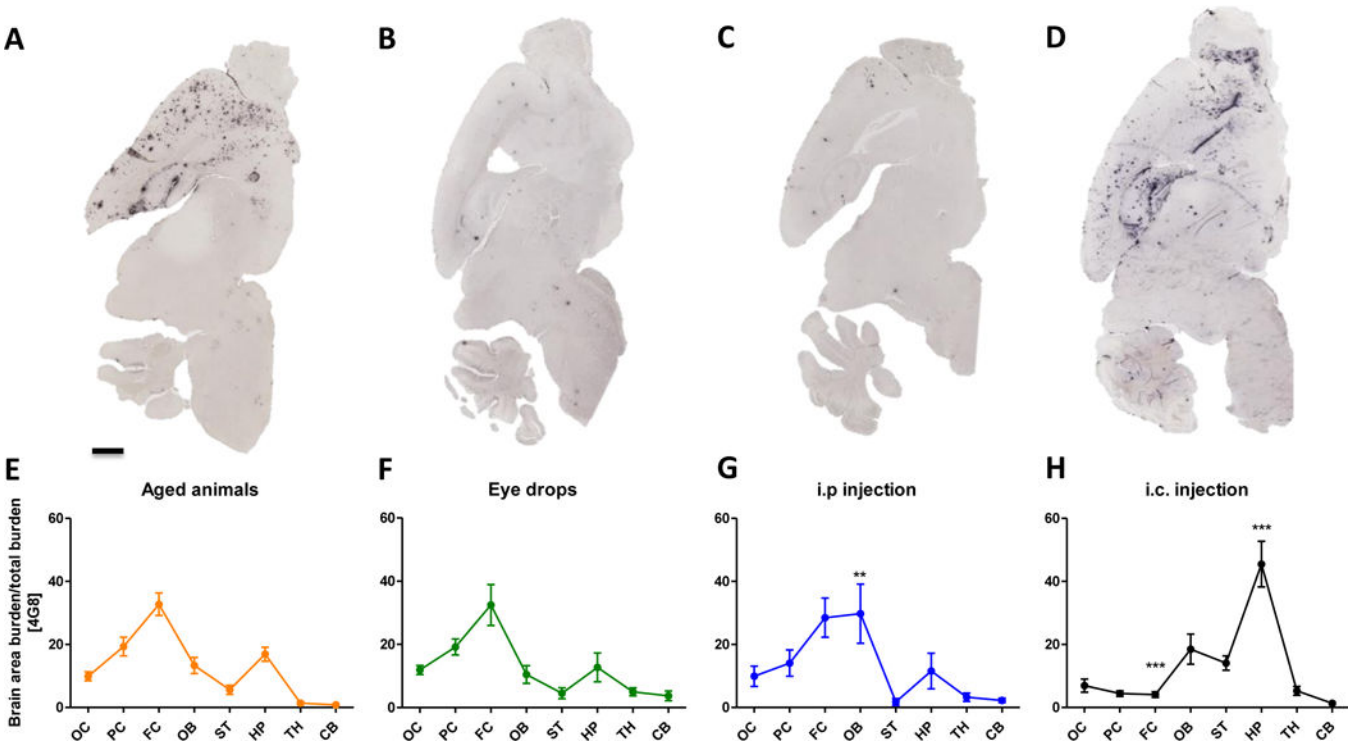

Figure 5. Regional profile of Aβ deposition in exogenously induced mice compared with untreated aged animals.

(A-D) Representative pictures of brain slices stained with the 4G8 antibody, highlighting Aβ deposition along the brain for experimental and control groups. Scale bar at the bottom of (A) represents 1,000 μm and applies to all panels. **(E-H)** The percentage of aggregation in different areas of the brain regarding total aggregation (%) was calculated by image analysis, as described in Materials and Methods. For (E-H), dots represent averages and vertical lines averages ± standard errors. Lines connecting dots were used to better visualize the pattern of aggregation in each group. **p < 0.01, ***p < 0.001. OC: occipital cortex; PC: parietal cortex; FC: frontal cortex; OB: olfactory bulb; ST: striatum; HP: hippocampus; TH: thalamus; CB: cerebellum.

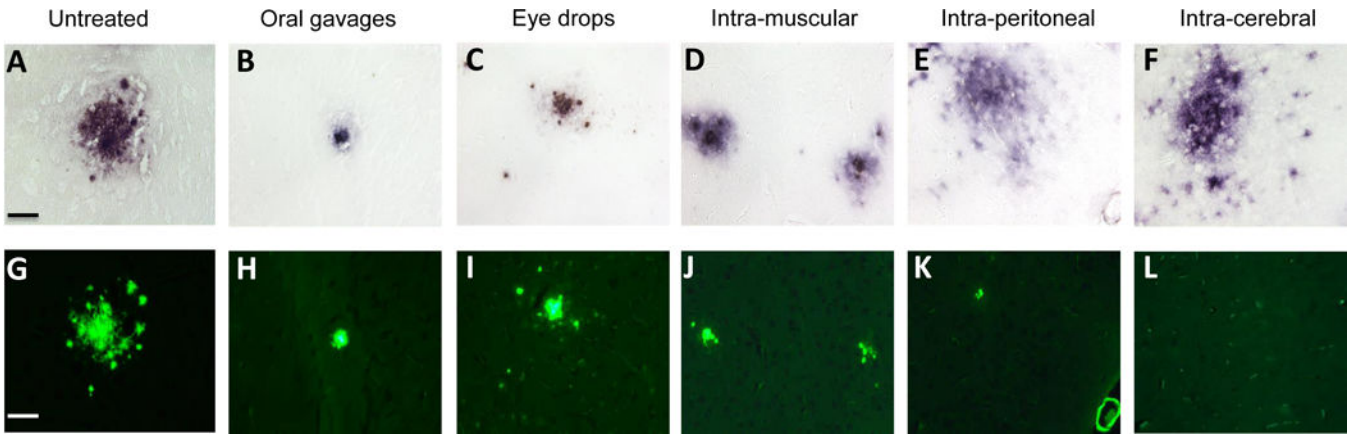

Figure 6. Morphological and staining differences in Aβ deposits induced by different routes of administration.

Consecutive brain slices for each experimental and control groups were stained with the 4G8 anti-Aβ antibody **(A-F)** and ThS **(G-L)**. Scale bars in (A) and (G) represent 100 μm and apply to all panels.

Table 1.

Estimated quantities of Aβ peptides injected by each route.

	n	Estimated amount of Aβ injected (ng)
Intra-cerebral	5	34.2
Eye drops	5	51.54
Intra-muscular	6	171.8
Intra-peritoneal	6	171.8
Oral gavages	4	1718
Untreated	6	--

Table 2.

Brain amyloidosis induced by brain and peripheral administration of misfolded Aβ.

	attack rate	Mean ± SD	fold	Age Equivalent (months, similar 4G8 burden)*	p value** (compared to untreated)
Intra-muscular	4/6	0.082 ± 0.047	11.77	13.98	0.0021
Eye drops	5/5	0.098± 0.0514	14.03	14.32	0.0009
Intra-peritoneal	6/6	0.205 ± 0.191	29.09	15.78	0.0146
Intra-cerebral	5/5	3.551 ± 1.019	507.28	>19	< 0.0001
Untreated	-	0.006961 ± 0.003237	1	-	-

*Data expressed in months for simplicity as untreated mice were sacrificed at the respective months with a ± difference of 5 days.

**Statistical differences in amyloid burden for each group were measured by Student's t-test with respect with the "Untreated" (negative control) group.